JOURNAL OF THERMOPHYSICS AND HEAT TRANSFER
Vol. 25, No. 1, January–March 2011

Processing and Characterization of Space-Durable High-Performance Polymeric Nanocomposite

H. M. S Iqbal,* S. Bhowmik,† and R. Benedictus‡
Delft University of Technology, 2629 HS Delft, The Netherlands
J. B. Moon§ and C. G. Kim¶
Korea Advanced Institute of Science and Technology, Daejon 305-701, Republic of Korea
and
A.-H. I. Mourad**
United Arab Emirates University, Al-Ain, United Arab Emirates

DOI: 10.2514/1.50841

In this investigation, efforts were given to develop carbon-nanofiber-reinforced polybenzimidazol nanocomposite for space application. Processing of polybenzimidazol was carried out by using polybenzimidazol in powder and solution forms. Thermomechanical properties of compression-molded polybenzimidazol, unfilled polybenzimidazol films, and nanofiber-reinforced polybenzimidazol films were investigated using thermogravimetric analysis, dynamic mechanical analysis, and tensile testing. Thermogravimetric analysis revealed that both compression-molded polybenzimidazol and polybenzimidazol films show high thermal stability. Dynamic mechanical analysis studies depicted that both compression-molded polybenzimidazol and polybenzimidazol neat films exhibited a high storage modulus, even at a temperature of 250°C. Polybenzimidazol nanocomposite films were cast with different loadings of carbon nanofibers from 0.5 to 2 wt % in polymer solution. Addition of carbon nanofibers improved the thermal stability and storage modulus of polybenzimidazol film. Mechanical testing showed that both compression-molded polybenzimidazol and polybenzimidazol films resulted in the highest ultimate tensile strength in comparison to any unfilled polymer. Investigation under scanning electron microscopy confirmed uniform dispersion of carbon nanofibers in polymer solution. Analysis of fractured surfaces revealed that neat polybenzimidazol film exhibited ductile failure and dispersion of carbon nanofibers into the polybenzimidazol, resulting in transformation from ductile to brittle failure.

I. Introduction

IN THE 21st century, it is well established that lightweight high-performance polymeric composites with excellent mechanical, thermal, and fatigue properties are of great interest for interplanetary space missions, especially to space structures, as applications of these materials reduce overall cost of the mission [1]. Despite these positive aspects of polymeric composite materials for space missions, for longer missions in which structures are required to undergo an extended period of time in a space environment, the polymer matrix shows limitation in maintaining the outstanding performance. Therefore, the present trend of research is primarily focused on development of a high-performance polymer with outstanding thermal and mechanical properties for extended exposure to a harsh space environment.

In this context, a newly emerged high-performance polymer such as polybenzimidazole (PBI) was processed and characterized. PBI is a heterocyclic thermoplastic polymer and shows excellent thermochemical properties and outstanding mechanical properties [2]. In molded form, PBI shows the highest compressive and tensile strength in comparison to any unfilled polymeric resin [3,4], as well as the highest glass transition temperature T_g (425°C), high decomposition temperatures (500–600°C), and stability under oxidation, and it maintains excellent strength at cryogenic temperatures [5]. PBI shows better strength than polyimide and polyamideimide at higher temperature and is also superior in terms of other properties such as chemical, radiation, and fire resistance, resulting in the best high-performance polymer for various applications to future-generation space [3]. The high thermal stability of PBI is attributed to the presence of aromatic and heterocyclic rings in the polymer chain, which provide rigidity to the polymeric chain [6]. Because of these properties, PBI is an excellent polymer for aviation and space applications. PBI has found its application for protective sealing, thermal and mechanical insulators, and nose cones of aircraft [3]. Because of its excellent thermal properties and superior non-flammability, PBI has been used for firefighters' protective clothing, high-temperature gloves, and astronauts' flight suits [7–9]. PBI has better insulating properties and it forms a good textile fiber [10]. In recent years, acid-doped PBI has emerged as a promising material for the application in the membrane of the fuel cell [10,11]. Having excellent thermal and chemical resistance and high mechanical properties, PBI has a great potential for space application as a heat-shielding and radiation-shielding material. It shows considerable promise not only as a matrix for high-temperature structural composite materials, but also as fibers and films [12].

Based on these considerations, an effort has been given in the present investigation to manufacture compression-molded PBI and PBI films with better thermal stability and high mechanical properties for space application. Despite having better thermal and mechanical properties, the real challenge is the processing of PBI as such, because this particular polymer does not melt. Moreover, compression-molded PBI requires very high temperature and metallurgical pressure to process. Therefore, very few research papers are available to date regarding the processing of PBI. Some researchers have demonstrated the processing of PBI in powder form

Received 19 May 2010; revision received 7 September 2010; accepted for publication 11 September 2010.

*Ph.D. Researcher, Chair Aerospace Materials and Manufacturing, Faculty of Aerospace Engineering, Kluyverweg 1.
†Senior Scientist, Chair Aerospace Materials and Manufacturing, Faculty of Aerospace Engineering, Kluyverweg 1. Member AIAA.
‡Professor, Chair Aerospace Materials and Manufacturing, Faculty of Aerospace Engineering, Kluyverweg 1.
§Ph.D. Researcher, Department of Aerospace Engineering.
¶Professor, Department of Aerospace Engineering.
**Associate Professor, Mechanical Engineering Department, Faculty of Engineering, P.O. Box 17555.

[13], and some other papers demonstrate the processing of PBI in *N*, *N*-dimethylacetamide (DMAc) solvent to produce PBI composite and nanocomposite [2,7,8]. In a previous study [7] about PBI nanocomposite, more emphasis was given on the mechanical properties of PBI/CNF (carbon nanofiber) nanocomposite. However, thermal properties of material were not studied in much detail. In this context, the present work has covered both thermal and mechanical aspects of compression-molded PBI and PBI/CNF nanocomposite. The study has demonstrated better thermomechanical properties of PBI nanocomposite films when compared to the results of the previous study. This study also has focused on process optimization of compression-molding PBI in detail.

Note that with the development of high-performance polymers, different nanofillers are also getting equal attention. The nanofillers are being incorporated to the polymer resins in order to further enhance their properties such as stiffness, toughness, thermal, and barrier [14]. CNFs receive significant attention for their potential applications as reinforcements in polymer matrices, due to their high tensile strength, modulus, and relatively low cost. Therefore, in this context, efforts were made to develop carbon-nanofiber-reinforced polymer nanocomposite films using different dispersion techniques; consequently, this paper opens a new window for dispersing nanofillers in PBI resins. Large research opportunities exist to answer more fundamental questions regarding dispersion, optimization of filler content, new potential applications, development of processing technologies, filler matrix interface interactions, and characterization techniques. The objective of this investigation is to prepare PBI/CNF composites by the film-casting technique and to examine their thermal and mechanical behaviors by using thermogravimetric analysis (TGA) and dynamic mechanical analysis (DMA), respectively. A detailed morphology analysis of fractured surfaces is presented by using scanning electron microscopy (SEM) to investigate failure mechanism, fiber dispersion, and CNF/matrix adhesion.

II. Experimental

A. Materials

High-temperature-resistant PBI thermoplastic with a density of 1.3 g/cm^3, having a molecular weight of 20,000 g/mole (Celazole brand, supplied by PBI Performance Products) was used for compression molding. A solution of PBI in DMAc (with 26% concentration of PBI, supplied by PBI Performance Products) was used for casting the film of neat PBI and PBI reinforced with CNFs. A solution of 99% concentrated *N*, *N*-DMAc was purchased from Aldrich Chemicals. Carbon nanofibers with diameters ranging from 70 to 200 nm and lengths of 50 to 200 μm were supplied by Pyrograf Products, Inc., with the trade name of PR-19-XT-LHT. All materials were used as received.

B. Processing of Polybenzimidazole

Compression molding of PBI powder was carried out using temperatures in excess of 400°C and high metallurgical pressure. To make the specimen using the compression-molding process and to get the best specimen with desired properties, different processing parameters were varied to optimize the process. Both heat and pressure were applied during the processing. Because PBI is not melt-processable sintering, a process used for metals is being used for the processing of PBI. In the sintering process, very high temperature and pressure are applied for long periods to compact the material together to give it the desired shape. The polymer is heated above its glass transition temperature before applying the high pressure to compact the material. The two different methods that were used to make the specimens using PBI powder follow.

1. Method 1

In this method, the mold was filled with the required amount of PBI powder and put in the press. The mold was heated to 440°C at a rate of 5°C/ min by applying a pressure of 10 MPa. The mold was kept at this pressure and temperature for 3 h. After 3 h, the mold was allowed to cool to a temperature of 50°C and then pressure was released and the molded part was removed.

2. Method 2

In this method, PBI powder was dried at 200°C for 12 h in a forced-air convection oven. After drying the PBI powder, the mold was filled and put in the press. The mold was heated to 440°C at a rate of 5°C/ min. It was kept at 440°C for 30 min to get a uniform heat distribution. Then a pressure of 55 MPa was applied on the mold with the same temperature for 4 h. Pressure was released for 30 s so that any gas formed during the heating process could escape. After 4 h, the mold was allowed to cool to a temperature of 100°C. At this point, the pressure was released and the molded part was removed.

C. Solution Casting of Basic PBI Film

In this process, efforts were given to fabricate PBI films using the PBI solution in DMAc. The PBI solution in DMAc was highly viscous, and therefore the solution was diluted by adding 10 ml of DMAc to 20 g of PBI solution. The resulting solution was stirred mechanically at 50°C for 15 min to get a uniform mixture of PBI in DMAc. The mixture was then used to produce films that were 60–80 μm thick. The films were prepared by spreading the mixture over the glass plate with the help of an adjustable doctor's blade. The film was allowed to dry in the vacuum oven at 80°C for 2 h and then it was cured at 200°C overnight. The cured film was peeled off from the glass plate by immersing in the hot distilled water at 80°C. The film was kept in hot distilled water for about 60 min to remove any lithium chloride that was added to the solution. After removing the film from the hot distilled water, there was a formation of wrinkles that might be due the presence of DMAc. There is also the possibility that lithium chloride could also be present to some extent. Therefore, in order to remove the wrinkles before mechanical testing, the film was pressed in the hot press at 250°C and at a pressure of 5 MPa. The film was again dried in the oven at 100°C for 4 h to remove any moisture, then it was dried in the vacuum oven overnight at 300°C to remove any DMAc present in the film.

D. Solution Casting of PBI Nanocomposite Films

To fabricate the nanocomposite film, mechanical stirring and bath sonication methods were used. In the first method, a precalculated amount of CNFs were carefully weighed and directly mixed in the diluted solution of PBI. The mixture was then stirred mechanically using an overhead stirrer at 300 rpm for 30 min. In another method, the calculated amount of CNFs was weighed and then added to the DMAc solvent and dispersed by ultrasonic mixing for 30 min at 60°C. After ultrasonic mixing, CNFs dispersed in DMAc solvent were added to the PBI solution. The ultrasonic process in combination with mechanical stirring was continued for the next 15 min. The mixture was then used to cast the film on the glass plate, as described in the previous section. The nanocomposite films were prepared by dispersing 0.5, 1, and 2 wt % of CNFs into the PBI matrix.

E. Thermal Gravimetric Analysis

TGA was carried out to determine thermal stability of PBI powder, compression-molded PBI, PBI neat film, and PBI nanocomposite film. Tests were performed using a Perkins Elmer thermal analysis instrument (Pyris Diamond Thermogravimetric Analyzer). Compression-molded samples were cut into small pieces using a cutter and then ground to get the small-size specimens for the TGA test. The weight of all the samples was maintained between 7 and 10 mg. The samples were heated from a temperature range of 25 to 600°C at a heating rate of 10°C/ min. The furnace was purged with nitrogen gas to prevent oxidation at a flow rate of 25 ml/ min.

F. Dynamic Mechanical Analysis

DMA is performed in tensile mode at an oscillation frequency of 1 Hz using Perkin-Elmer dynamic mechanical analyzer (Pyris Dynamic Mechanical Analyzer). Samples of compression-molded

PBI were cut into a rectangular shape and then machined to the final dimensions of $1.2 \times 8.1 \times 40$ mm^3. PBI neat film and nanocomposite films were cut in rectangular form with dimensions of $0.06 \times 8 \times 40$ mm^3. Data are collected from 25 to 550°C at a scanning rate of 3°C/ min. Elastic modulus and mechanical damping of all the samples were measured.

G. Tensile Testing

Tensile testing of compression-molded PBI, neat PBI film, and nanocomposite films was carried out using a Zwick Tensile machine at a test speed of 2 mm/ min at 20°C. Rectangular specimens of $150 \times 10 \times 0.06$ mm^3 were cut from the cast films. Compression-molded specimens were machined to dumbbell shape for tensile testing. Five specimens for each material were tested for the reproducibility of the results. Force-displacement curves were recorded from which Young's modulus and tensile strength were evaluated. An extensometer was also used to determine the exact value of Young's modulus.

H. Fractographic Analysis

SEM studies were carried out on gold-coated films in order to examine the dispersion of carbon nanofibers in the polymer matrix and to study the fracture surfaces after mechanical testing. Images were obtained using a JEOL JSM-7500F field emission SEM.

III. Results and Discussion

A. PBI Processing

Compression molding of PBI powder was carried out using temperature in excess of 400°C and high metallurgical pressure. The aim of this investigation was to prepare specimens with high tensile strength as reported by the supplier of PBI. Two methods were applied to manufacture the specimen using the compression-molding process. In the first method, PBI powder was heated up to 440°C at a pressure of 10 MPa by keeping the mold at this temperature for 3 h. The specimen obtained after compression molding is shown in Fig. 1a. The specimen looks foamy, which might be due to low pressure during compression molding, which results in incomplete compactness of the material. Therefore, proper temperature and pressure should be applied in order to soften the material and to get enough compaction of the material so that it can achieve the desired strength.

In the second method, before compression molding, the material was sufficiently dried in order to avoid any moisture (which may result in voids in the molded specimen), and a high pressure of 55 MPa was applied, as recommended by the manufacturer of PBI. The heating cycle was also increased from 3 to 4 h. The specimen obtained with this method is shown in Fig. 1b. In this case, the specimen shows improvement of compactness and density of the material. The reason behind maintaining the mold at high temperature and pressure for a longer time was that the PBI is an amorphous thermoplastic and it does not melt, even at high temperature. However, PBI shows a softening point: i.e., a glass transition temperature at which molecules are flexibility enough and the desired shape can be given. Therefore, sintering is the only process for fabrication of these materials where high temperature and pressure are applied to the material to get the desired shape.

B. Processing of PBI Neat Film and Nanocomposite Film

PBI in the form of film was produced to evaluate thermal and mechanical properties of the polymer. Figure 2a represents neat PBI film obtained from solution casting. After removing the film from the glass plate using hot distilled water, wrinkles were formed, which were removed by pressing the film in the hot press at 250°C and at a pressure of 5 MPa. PBI nanocomposite films obtained with two different dispersion techniques having 1 wt % of CNFs are shown in Figs. 2b and 2c, and the compression-molded specimen is shown in Fig. 2d. The nanocomposite film obtained with separate dispersions of CNFs in DMAc solvent using ultrasonication is shown in Fig. 2b. After dispersion of nanofibers in the polymer solution, the color of the film was totally changed from brown, as in the case of neat PBI film, to blackish, which could be the first test of examining the uniform dispersion of CNFs in the polymer matrix. In the case of PBI nanocomposite film that was obtained by direct mechanical mixing of CNFs into the polymer solution, the dispersion of CNFs is not up to the mark, as evident from Fig. 2c.

The color of the film was not changed and agglomeration of CNFs is clearly observed. Therefore, it can be concluded that ultrasonication of CNFs before adding into the polymer solution is the more effective way to get PBI nanocomposite films.

C. Thermal Gravimetric Analysis

TGA of PBI powder, compression-molded PBI, PBI neat film, and PBI nanocomposite film was carried out to determine the thermal stability of the polymer. Figure 3a represents a comparison of PBI polymer in different forms. TGA curves show the thermal decomposition behavior of polymer as a function of temperature. The decomposition behavior of PBI powder is shown in Fig. 3a. The TGA curve shows two-step decomposition. The initial weight loss that occurred between 40 and 130°C is around 2.35%. This weight loss occurred due to evaporation of water. PBI is highly hygroscopic; therefore, it absorbs moisture that evaporates during heating, resulting in a reduction in weight. The weight loss at the initial stage can be minimized by drying the powder in the oven. After the first degradation step, weight loss starts very slowly but continuously until the temperature reaches 545°C. There is only a 5% weight loss up to this temperature, which is significantly lower than with other polymers. Therefore, it can be concluded that thermal stability of PBI is superior in comparison to any other polymer. The high thermal stability of PBI is due to the presence of aromatic and heterocyclic rings in the polymer chain. The loss in weight in the second degradation step was due to the loss of phenol and other gaseous products, which is confirmed by experiments [15]. At very high temperature, ammonia and methane evolved from heterocyclic and aromatic rings, respectively.

Comparative studies of thermal decomposition behavior of compression-molded PBI with PBI powder reveals that compres-

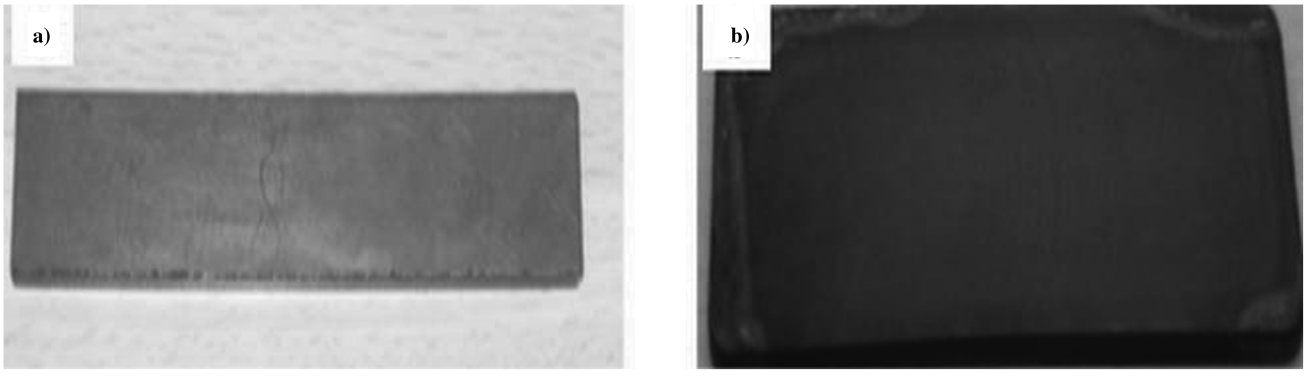

Fig. 1 Photographs of a) compression-molded at low pressure and b) compression-molded at high pressure.

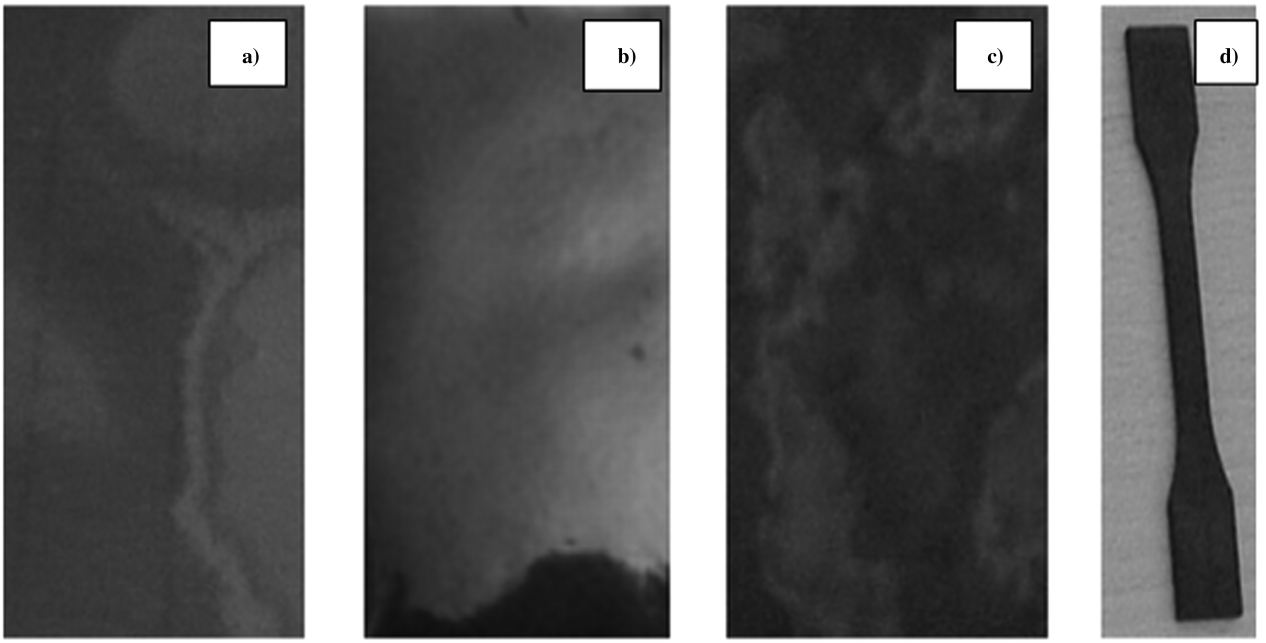

Fig. 2 Photographs of a) PBI neat film, b) PBI 1 wt % CNF obtained after ultrasonication of the solution, c) PBI 1 wt % CNF obtained after direct mechanical mixing, and d) compression-molded PBI sample.

sion-molded PBI shows high thermal stability at the initial stage, up to a temperature range of 200°C. The high thermal stability of compression-molded specimen might be due to its exposure to the high temperature during the compression-molding process. High temperature dries the material and removes moisture that was present in PBI powder. On the other hand, for compression-molded PBI, the weight loss occurred continuously up to a temperature of 325°C without any stable plateau. After this temperature, the polymer exhibits thermal stability, and only 0.2% weight loss occurred from a temperature of 400 to 550°C, with a total weight loss of 6.5% up to this temperature, which is still high thermal stability of polymer at this temperature. The continuous weight loss of the PBI polymer in the first stage could be explained with the fact that exposure of PBI to the surrounding air at high temperature during the compression-molding process might have oxidized the material, which ultimately degraded the material properties to some extent.

The TGA curve for neat PBI film and PBI nanocomposite film is shown in Fig. 3b. The TGA curve shows two-step degradation for neat PBI film. A relatively short degradation step started at about 50°C and continued up to 150°C, with a 2% weight loss. The weight loss occurred due to absorption of moisture by the polymer, and any DMAc remained inside the polymer film, even when it was dried. After the first degradation step, the weight loss occurred gradually but very slowly. The polymer remained stable until the temperature of 405°C, with a total weight loss of 5%; thereafter, the second degradation step started, where weight loss occurred more rapidly, but PBI was not totally degraded. Only a 9.5% weight loss occurred up to the temperature of 600°C. The addition of 1 wt % of CNFs in PBI has not improved the thermal stability of PBI in the first degradation step, but an improvement is observed at higher temperature, and a 5% weight loss occurred at a temperature of 420°C, with 0.5 wt % CNFs in the polymer. After the addition of 2% carbon nanofibers in the polymer, it was observed that thermal stability of PBI improved remarkably. The first step of degradation has been almost eliminated, as most of the moisture has been absorbed by CNFs. There is only a 1.2% weight loss observed up to

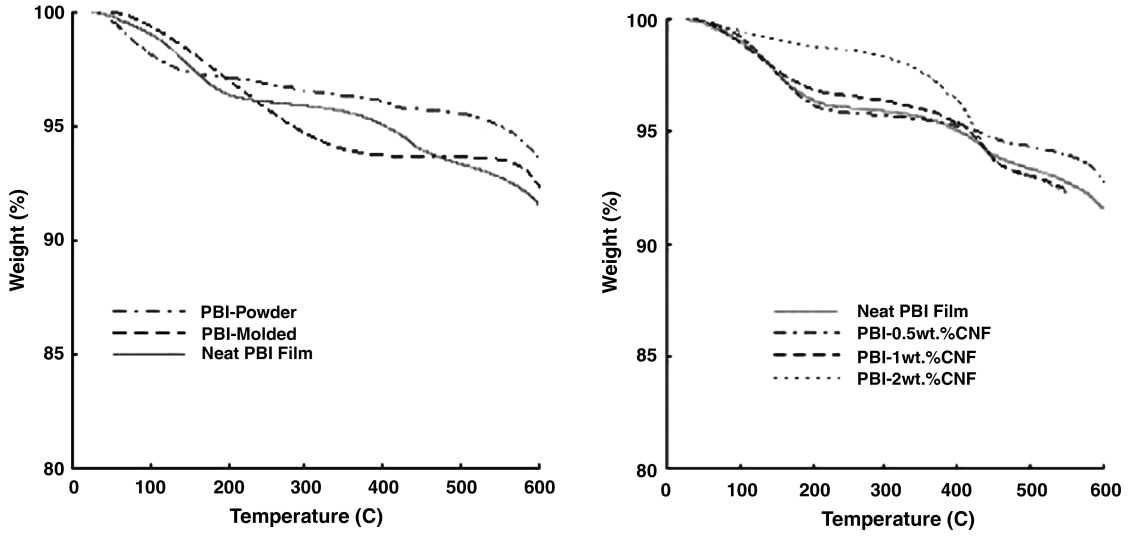

a) b)

Fig. 3 Plots of comparison of thermal stability of PBI: a) in different forms and b) neat film and nanocomposite film.

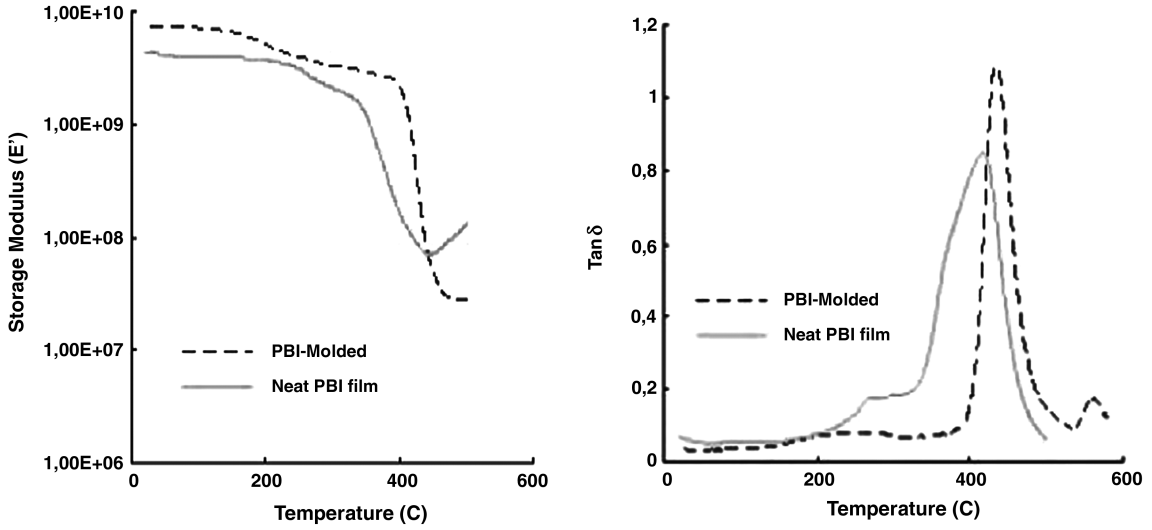

a) b)

Fig. 4 Comparison of a) storage modulus and b) loss-factor curve of compression-molded PBI and PBI films.

the temperature of 200°C, and then the polymer remained stable up to the temperature of 430°C, with 5% of weight loss; thereafter, the polymer started to degrade. This is because high thermal stability with 2 wt % CNFs could lead to high cross-linking density at this loading. Cross-linking restricts mobility of the polymeric chains, which ultimately delays the decomposition of the materials. A previous study [16] on CNF-reinforced polymer composite has revealed that reinforcement of CNFs, even with small weight percent, improve the thermal conductivity of the material. Therefore, it is also expected for this study that thermal conductivity of the polymer has improved specifically with 2 wt % loading of CNFs, which could be the reason that by dispersing 2 wt % CNFs, thermal stability of the material has improved, as heat dissipates more quickly at 2 wt % loading of CNFs.

D. Dynamic Mechanical Analysis

DMA is performed in tensile mode at a fixed frequency of 1 Hz to study the behavior of storage modulus E' as a function of temperature and glass transition temperature T_g. A comparison of storage modulus for molded PBI and PBI neat films is shown in Fig. 4a. The figure reveals that the compression-molded specimen shows a high storage modulus throughout the temperature range in comparison to the storage modulus of the PBI film. One of the explanations of the low storage modulus of PBI neat film could be the DMAc solvent that could be present in the film. The presence of DMAc solvent might have reduced the stiffness of the PBI film. When comparing the loss-factor curve of compression-molded PBI and PBI films, it is observed that compression-molded PBI shows high glass transition and it is at 430°C, as shown in Fig. 4b. However, PBI film indicates a wider loss-factor curve, resulting in better cross-linking of the PBI film.

DMA plots of the storage modulus as a function of temperature for both neat PBI film and PBI nanocomposite film at different carbon nanofiber loadings are shown in Fig. 5a. The figure demonstrates that addition of 0.5 wt % of CNFs increases the storage modulus up to 88% (from 4.26 to 8.03 GPa). By further adding CNFs in polymer up to 2 wt %, a small decrease in storage modulus is observed, but this value is still higher than the storage modulus of the neat PBI film. A 50% increase in the storage modulus from 4.26 to 6.41 GPa is observed with 2 wt % of CNFs, and this is relatively higher than that reported in literature [7]. By adding CNFs to the polymer, the improvement in the first plateau of the storage modulus is observed

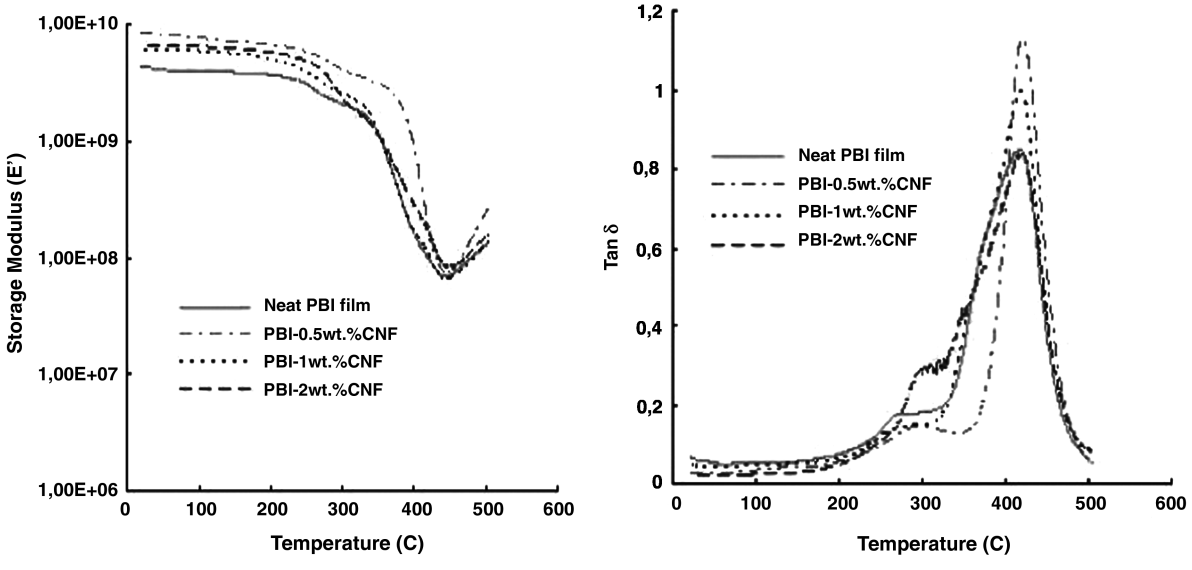

a) b)

Fig. 5 Comparison of a) storage modulus and b) loss-factor curve of neat PBI film and PBI nanocomposite films.

Table 1 Storage modulus of compression-molded PBI, PBI neat film, and nanocomposite film as a function of temperature

Materials	$E'_{30°C}$, GPa	$E'_{100°C}$, GPa	$E'_{200°C}$, GPa	$E'_{250°C}$, GPa	$E'_{300°C}$, GPa	$E'_{350°C}$, GPa	$E'_{400°C}$, GPa	Glass transition temperature, T_g [a]
Compression-molded PBI	6.95	6.85	4.93	3.81	3.18	2.84	2.13	434
Neat PBI Film	4.26	3.93	3.70	3.12	2.08	1.20	0.16	416
PBI-0.5% CNF nanocomposite film	8.03	7.43	6.47	5.58	3.96	2.99	0.74	421
PBI-1% CNF nanocomposite film	5.85	5.68	4.91	3.81	2.47	1.14	0.16	418
PBI-2% CNF nanocomposite film	6.41	6.25	5.55	4.63	2.26	1.04	0.27	419

[a]Glass transition onset of peak of loss-factor curve.

and a drop of storage modulus of nanocomposite films occurs at certain higher temperatures when compared to the neat PBI film. The decrease in the storage modulus after the first plateau is typically related to the small movement of polymer molecules in the side chains. This is the typical characteristic of an amorphous polymer, which shows two plateaus in the storage modulus and then there is a sharp decrease in the storage modulus. The sharp decrease in the storage modulus after the second plateau is due to the large movement of the molecules in the polymer backbone that cause the material to soften and thus cause a decrease in stiffness of the polymer. A summary of the storage modulus at different temperatures is presented in Table 1.

Comparing the results for this study and results presented previously [7], it can be observed that PBI neat film and nanocomposite films have shown higher values of storage modulus, Young's modulus, and tensile strength for this study when compared with the results of the previous study [7]. One of the possible explanations of achieving better results could be the better fiber–matrix interface. Proper adhesion between fiber and matrix is essential in order to ensure optimum stress transfer across the resulting interfaces [17,18]. Another possible explanation could be the higher cross-linking of polymer films manufactured in this study. Cross-linking restricts the motion of the polymeric chains and results in an improved value of storage modulus and strength of polymer. Therefore, it can be concluded that better processing of PBI film is achieved in this investigation.

The loss-factor curve of the neat PBI film and PBI nanocomposite measured by DMA is shown in Fig. 5b. The curve represents two transition peaks at different temperatures. The higher temperature transition is normally referred to as glass transition T_g, which occurs when the main polymer chains are free to rotate, and is associated with a substantial fall in mechanical strength. The peak height of loss factor increased and became narrower by adding 0.5 wt % of carbon nanofibers. By further adding carbon nanofibers, a decrease in peak height of loss-factor curve was observed. However, there was a broadening of the peak in the loss-factor curve, which was due to the unconstrained segment of polymer molecules. Table 1 represents the glass transition temperature measurement as an onset of maximum peak height of loss-factor curve. Both neat PBI and PBI nanocomposite have very high glass transition temperatures, as reported in the table. A secondary transition, called β transition, was also observed in the loss-factor curve of neat PBI and PBI nanocomposite. This transition represents the motions of side chain molecules in the polymer. It was observed that by adding carbon nanofibers in the polymer, the value of secondary transition temperature increased up to 30°C, with 2 wt % of carbon nanofibers. Carbon nanofibers restricted the motion of the side chain molecules very effectively.

E. Tensile Testing

Tensile tests of molded PBI, neat PBI film, and PBI nanocomposite to study the effect of CNFs on tensile properties of PBI were performed using a Zwick tensile machine at room temperature with a test speed of 5 mm/ min. A comparison of tensile test results with each material is presented in Table 2. A tensile strength of 112 MPa was obtained with the compression-molded specimen processed at a temperature of 440°C with a pressure of 10 MPa. Compression-molding of PBI at a temperature of 440°C and at a pressure of 55 MPa resulted in a tensile strength of 145 MPa, and it is clearly the highest tensile strength of any unfilled polymer. In this case, note that the PBI powder was dried in a vacuum oven for 12 h before the compression-molding process.

In the first case, it is possible that as the PBI powder was not dried, resulting in the presence of moisture during curing, leading to low tensile strength. Also, the temperature, pressure, and heating cycle during the compression molding were not optimized enough to get the full strength of the molded material. During this process, since pressure is applied to the PBI resin continuously during heating, the decomposed gas resulting from the heating of PBI could not escape from the sintered PBI and therefore remains therein as voids. These voids cause the cracking of the specimen, resulting in the decrease of tensile strength. The decomposed gas comprises the vapor resulting from the decomposition of the nonpolymerized PBI resin itself and the vapor resulting from the reaction of lithium chloride (this is added to the PBI resin as a stabilizer) with the PBI resin at high temperatures. The decomposed gas includes CO, CO_2, CH_4, chloroform, and phenol [15]. Therefore, in conclusion, the temperature, pressure, and heating cycle need to be selected carefully.

Tensile strength and Young's modulus of PBI neat film and PBI nanocomposite film are illustrated in Fig. 6. A tensile strength of 157 MPa is achieved for neat PBI film. Further increase in strength is observed by adding 1 and 2% CNFs in the polymer, as shown in Fig. 6. A 9% increase in tensile strength is achieved by dispersing 1% CNFs in the PBI.

Note that both stiffness and toughness of PBI have also increased. By adding CNFs up to 2 wt %, a further increase in tensile strength of PBI film is observed. In this case, a 15% increase in tensile strength is observed and the value of Young's modulus has increased from 6.55 to 8.11 GPa, an improvement of about 24%, as shown in Fig. 6. An improvement of 30% in failure strain is also observed by adding 2%

Table 2 Tensile test results for compression-molded PBI, PBI neat film and PBI nanocomposite film

Materials	Tensile strength [c], MPa	Tensile modulus, GPa	Elongation, %	Std. dev.
Compression-molded PBI-1 [a]	112	5.63	1.56	6.34
Compression-molded PBI-1 [b]	145	7.77	1.96	6.46
Neat PBI film	157	6.55	2.67	3.1
PBI-0.5% CNF nanocomposite film	165	7.02	2.90	4.18
PBI-1% CNF nanocomposite film	171	7.77	3.25	4.27
PBI-2% CNF nanocomposite film	181	8.11	3.46	5.93

[a]Compression-molded specimens produced by simultaneous heating and pressing of PBI powder at low pressure.
[b]Compression-molded specimens produced by simultaneous heating and pressing of PBI powder at high pressure.
[c]Results are the average of six replicate specimens.

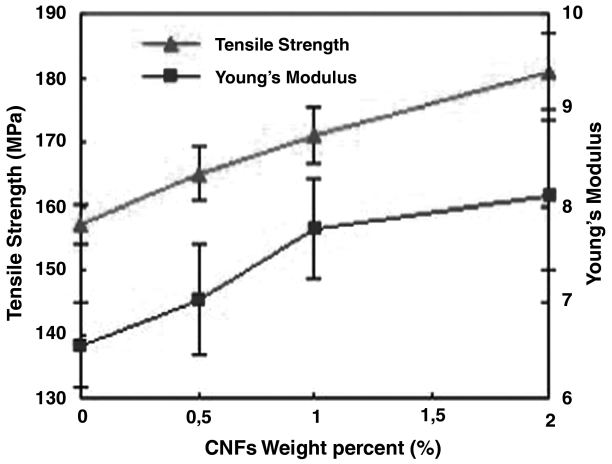

Fig. 6 Comparison of tensile strength and Young's modulus of PBI neat film and nanocomposite film with different CNF loadings.

CNFs in PBI polymer. In general, filler additions are detrimental to the toughness of the material. However, it is interesting to see that the addition of carbon nanofibers has improved the toughness of PBI. This kind of effect of CNFs on the toughness of the polymer has also been reported by some other researchers [6,7].

F. Scanning Electron Microscope Analysis

Scanning electron microscopy of neat PBI and PBI nanocomposite was carried out to examine the dispersion of carbon nanofibers. Though carbon nanofibers are difficult to disperse in the polymer matrix due to large surface area, SEM analysis of the samples for the case when the fibers were first ultrasonicated in DMAc and then dispersed in PBI has shown good dispersion of CNFs with all the fiber loadings. However, the samples with 2 wt % of CNFs have shown very few agglomerations, as shown in Fig. 7c.

Samples prepared by direct mixing of 1 wt % of carbon nanofibers into the polymer matrix have shown a large agglomeration area, as shown in Fig. 7d. Direct mixing of carbon nanotubes into the PBI polymer was studied by Okamoto et al. [8] and good dispersion of CNTs into the PBI polymer was reported.

G. Fracture Morphology

Scanning electron microscopy was also carried out to examine the fracture morphology of failed surfaces after tensile testing of neat PBI, PBI nanocomposite film, and compression-molded PBI. A ductile failure was observed for neat polymer film, as shown in Fig. 8a. The fracture surface shows a wavelike pattern that might be due to the plastic yielding that occurred locally while the load was applied. By adding 0.5 wt % of CNFs in the polymer matrix, a mixed kind of failure was observed and a phase transition appeared from ductile to brittle failure. Analyzing the fracture surfaces of nanocomposite film reinforced with 2 wt % of CNFs, it is observed that deformation occurred in a different direction, as crack growth is limited to one direction, due to the fibers present in the matrix.

A much rougher fracture surface was observed upon adding 2 wt % CNF into the PBI matrix, as shown in Fig. 8c. The increased surface roughness implies that the path of the crack tip is distorted because of the carbon nanofiber, making crack propagation more difficult. CNFs act as a crack arrestor and delayed the crack

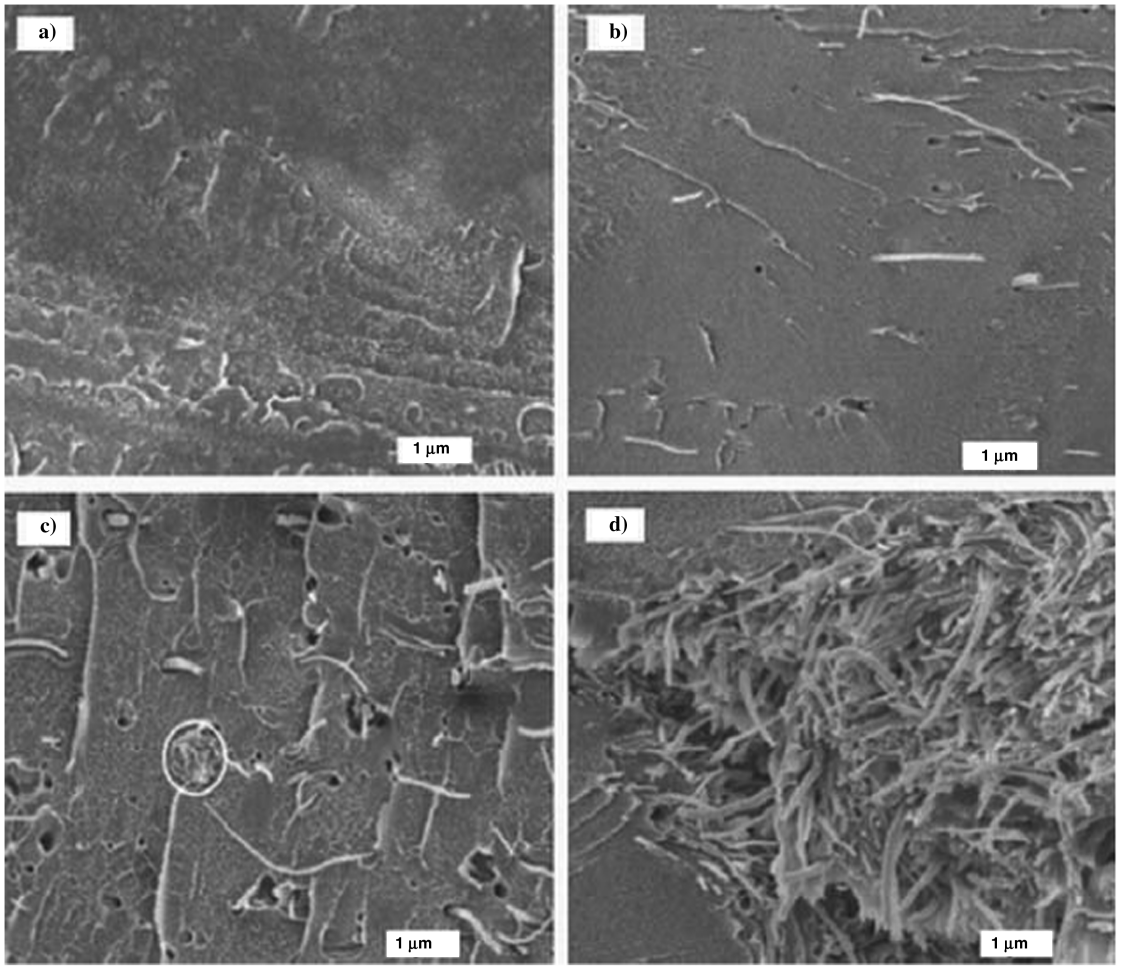

Fig. 7 SEM analyses of PBI neat film and nanocomposite film with different nanofiber loadings: a) neat PBI film, b) PBI 0.5 wt % CNFs ×3000, c) PBI 2 wt % CNFs ×3000, and d) PBI 1 wt % CNFs ×3000 produced with direct mixing of CNFs into the polymer solution.

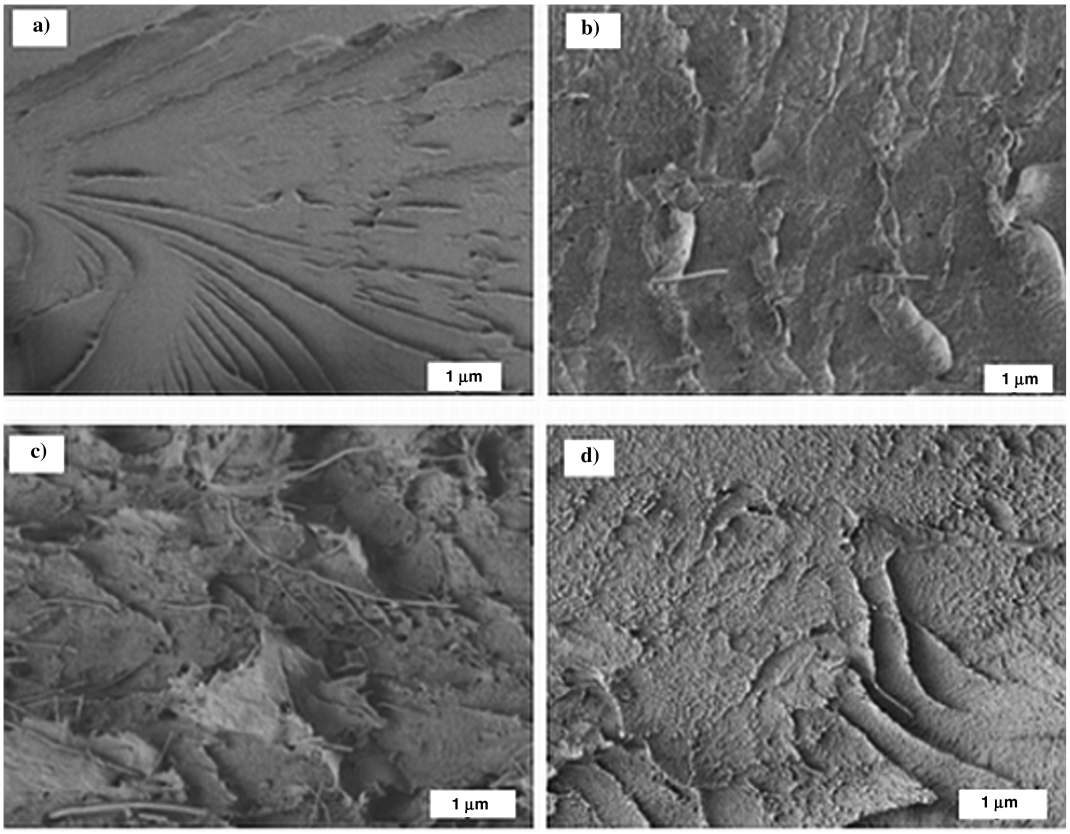

Fig. 8 SEM micrographs of fractured surface of PBI neat film and nanocomposite film with different nanofiber loadings and compression-molded PBI: a) neat PBI film, b) PBI 0.5 wt % CNFs ×3000, c) PBI 2 wt % CNFs ×3000, and d) compression-molded PBI.

propagation in the matrix material. Because of more resistance to crack growth in the presence of CNFs, both strength and stiffness of nanocomposite have increased when compared to neat PBI film, as indicated by the results in Table 2. Better interfacial adhesion of CNFs with the matrix material is essential in order to gain the benefit of CNFs. Absence of an effective interface between the carbon nanofiber and the neat resin does not help to transfer the mechanical loads between the two regions.

Fracture surface of compression-molded PBI is shown in Fig. 8d. Compression-molded specimens also have a similar kind of fracture morphology as that demonstrated by PBI basic film: ductile failure of the material.

IV. Conclusions

Thermomechanical properties of both compression-molded PBI, PBI neat film, and nanocomposite films were investigated using thermogravimetric analysis (TGA), dynamic mechanical analysis (DMA), and tensile testing. TGA analysis showed that compression-molded PBI has very high thermal stability up to a temperature of 550°C. Thermal stability of PBI film improved about 15% by loading up to 2% CNFs. DMA studies showed that both compression-molded PBI and PBI neat films exhibit very high storage modulus of 3.81 and 3.12 GPa, respectively, even at a temperature of 250°C, and a further improvement of about 48% was observed after the addition of 2% CNFs in PBI solution. Ultimate tensile strengths of compression-molded PBI and PBI films were 145 and 157 MPa, respectively. A considerable improvement in tensile strength of about 15% was achieved by dispersing 2 wt % of CNFs in PBI film. Scanning electron microscopy has confirmed the uniform dispersion of CNFs in polymer solution. Analysis of fractured surfaces revealed that a ductile failure occurred for neat PBI film and for nanocomposite; the failure was translated from ductile to brittle. These results lead to the conclusion that PBI is a high-performance polymer with excellent thermal and mechanical properties, and these properties make PBI an excellent candidate for aerospace applications.

References

[1] Han, J.-H., and Kim, C.-G., "Low Earth Orbit Space Environment Simulation and Its Effects on Graphite/Epoxy Composites," *Composite Structures*, Vol. 72, No. 2, 2006, pp. 218–226. doi:10.1016/j.compstruct.2004.11.007

[2] Steinerand, P. A., and Sandor, R., "Polybenzimidazole Prepreg: Improved Elevated Temperature Properties with Autoclave Processability," *High Performance Polymers*, Vol. 3, No. 3, 1991, pp. 139–150. doi:10.1088/0954-0083/3/3/001

[3] Kemmish, D. J., *High Performance Engineering Plastics*, Rapra Review Reports, Vol. 86, Rapra Technology, Shrewsbury, England, U. K, 1995.

[4] Beland, S., *High Performance Thermoplastic Resins and Their Composites*, 1st ed., Noyes Data Corp., Park Ridge, NJ, 1990, pp. 47–50.

[5] Bhowmik, S., Bonin, H. W., Bui, V. T., and Weir, R. D., "Modification of High-Performance Polymer Composite Through High-Energy Radiation and Low-Pressure Plasma for Aerospace and Space Applications," *Journal of Applied Polymer Science*, Vol. 102, Jan. 2006, pp. 1959–1967. doi:10.1002/app.24230

[6] Smay, G. L., "The Characteristics of High-Temperature Resistant Organic Polymers and the Feasibility of Their Use as Glass Coating Materials," *Journal of Material Science and Technology (Sofia)*, Vol. 20, No. 4, 1985, pp. 1494–1500. doi:10.1007/BF01026347

[7] Zhang, L., Ni, Q.-Q., Shiga, A., Fu, Y., and Natsuki, T., "Synthesis and Mechanical Properties of Polybenzimidazole Nanocomposites Reinforced by Vapor Grown Carbon Nanofibers," *Polymer Composites*, Vol. 31, No. 3, 2009, pp. 491–496. doi:10.1002/pc.20829

[8] Okamoto, M., Fujigaya, T., and Nakashima, N., "Individual Dissolution of Single-Walled Carbon Nanotubes by Using Polybenzimidazole, and Highly Effective Reinforcement of Their Composite Films," *Advanced Functional Materials*, Vol. 18, No. 12, 2008, pp. 1776–1782. doi:10.1002/adfm.200701257

[9] Sidman, K. R., and Gregory, J. B., "Development of Thermally Stable Polybenzimidazole (PBI) Fiber," Aeronautical Systems Div., TR 72-50, Nov. 1971.

[10] Sannigrahi, A., Arunbabu, D., Sankar, M., and Jana, T., "Tuning the Molecular Properties of Polybenzimidazole by Copolymerization," *Journal of Physical Chemistry B*, Vol. 111, No. 42, 2007, pp. 12124–12132.
doi:10.1021/jp073973v

[11] Hel, R., Li, Q., Bach, A., Jensen, J. O., and Bjerrum, N. J., "Physicochemical Properties of Phosphoric Acid Doped Polybenzimidazole Membranes for Fuel Cells," *Journal of Membrane Science*, Vol. 277, 2006, pp. 38–45.
doi:10.1016/j.memsci.2005.10.005

[12] "Fibrous Reinforcement for Space Applications," NASA CR-796, 1967.

[13] Hughes, O. R., Chen, O. N., Cooper, W. M., Disano, L. P., Alvarez E., and Andres, T. E., "PBI Powder Processing to Performance Parts," *Journal of Applied Polymer Science*, Vol. 53, No. 5, 1994, pp. 485–496.
doi:10.1002/app.1994.070530503

[14] Gojny, F. H., Wichmann, M. H. G., Fiedler, B., and Schulte, K., "Influence of Different Carbon Nanotubes on the Mechanical Properties of Epoxy Matrix Composites—A Comparative Study," *Composites Science and Technology*, Vol. 65, Nos. 15–16, 2005, pp. 2300–2313.
doi:10.1016/j.compscitech.2005.04.021

[15] Kurisaki, M., and Sasaki, Y.,, "Process for Manufacturing Sintered Polybenzimidazole Article," U.S. Patent 5770142, filed 13 June 1997.

[16] Moore, A. L., Cummings, A. T., Jensen, J. M., Shi, L., and Koo, J. H., "Thermal Conductivity Measurements of Nylon 11-Carbon Nanofiber Nanocomposites," *Journal of Heat Transfer*, Vol. 131, No. 9, 2009, p. 5.
doi:10.1115/1.3139110

[17] Lafdi, K., Fox, W., Matzek, W., and Yildi, E., "Effect of Carbon Nanofiber-Matrix Adhesion on Polymeric Nanocomposite Properties: Part II," *Journal of Nanomaterials*, Vol. 2008, July 2008, Paper 310126.
doi:10.1155/2008/310126

[18] Bradley, R. H., "Interfacial Studies of Carbon Fiber Reinforced Composites," *Key Engineering Materials*, Vols. 99–100, 1995, pp. 37–42.
doi:10.4028/www.scientific.net/KEM.99-100.37